REPORT DOCUMENTATION PAGE

Form Approved
OMB No. 074-0188

1. AGENCY USE ONLY (Leave blank)	2. REPORT DATE	3. REPORT TYPE AND DATES COVERED
	24-26 Oct. 1995	Technical Report, 24-26 Oct. 1995

4. TITLE AND SUBTITLE
Detection and Retrieval of Cirrus Cloud Systems Using AVHRR Data: Verification Based on Fire-II-IFO Composite Measurements

5. FUNDING NUMBERS
Air Force Geophysic Directorate
Contract F19628-95-K-002

NASA Grants NAG5-1050
NAG1-1719

6. AUTHOR(S)
K.N. Liou, S.C. Ou, N.X. Rao, and Y. Takano

7. PERFORMING ORGANIZATION NAME(S) AND ADDRESS(ES)

University of Utah
Department of Meteorology/CARSS
Salt Lake City, Utah 84112

8. PERFORMING ORGANIZATION REPORT NUMBER
N/A

9. SPONSORING / MONITORING AGENCY NAME(S) AND ADDRESS(ES)
SERDP
901 North Stuart St. Suite 303
Arlington, VA 22203

10. SPONSORING / MONITORING AGENCY REPORT NUMBER
N/A

11. SUPPLEMENTARY NOTES
Published in the proceedings of the Cloud Impacts on DoD Operations and Systems 1995 Conference (CIDOS-95). This work was supported in part by Air Force Geophysics Directorate under Contract No. F19628-95-K-002, and by NASA under Grants No. NAG5-1050 and NAG1-1719. The United States Government has a royalty-free license throughout the world in all copyrightable material contained herein. All other rights are reserved by the copyright owner.

12a. DISTRIBUTION / AVAILABILITY STATEMENT
Approved for public release: distribution is unlimited

12b. DISTRIBUTION CODE
A

13. ABSTRACT ***(Maximum 200 Words)***

A detection scheme to identify single and multilayer cirrus cloud systems was developed based on the physical properties of the AVHRR Ch.1-2 reflectances and ratios.

14. SUBJECT TERMS
AVHRR, FIRE-II-IFO, NCAR-CLASS, SERDP, cirrus, cloud detection

15. NUMBER OF PAGES
5

16. PRICE CODE
N/A

17. SECURITY CLASSIFICATION OF REPORT	18. SECURITY CLASSIFICATION OF THIS PAGE	19. SECURITY CLASSIFICATION OF ABSTRACT	20. LIMITATION OF ABSTRACT
unclass	unclass	unclass	UL

CLOUD IMPACTS ON DOD OPERATIONS AND SYSTEMS 1995 CONFERENCE

U.S. Air Force Phillips Laboratory – Science Center
Hanscom Air Force Base, Massachusetts
24-26 October 1995

CIDOS – 95

Cloud Modeling and Data for Defense Simulation Activities

"Emphasizing Sufficient Physical Reality in Simulating Clouds"

PL-TR-95-2129
Environmental Research Papers, No. 1179

PREPRINT OF THE CLOUD IMPACTS ON DoD OPERATIONS AND SYSTEMS 1995 CONFERENCE (CIDOS–95)

Editor

Donald D. Grantham

1 October 1995

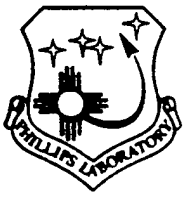

PHILLIPS LABORATORY
Directorate of Geophysics
Air Force Materiel Command
Hanscom Air Force Base, MA 01731-3010

DETECTION AND RETRIEVAL OF CIRRUS CLOUD SYSTEMS USING AVHRR DATA: VERIFICATION BASED ON FIRE-II-IFO COMPOSITE MEASUREMENTS

K.N. Liou, S.C. Ou, N.X. Rao, and Y. Takano
University of Utah
Department of Meteorology/CARSS
Salt Lake City, Utah 84112

ABSTRACT

We have developed a detection scheme to identify single and multilayer cirrus cloud systems based on the physical properties of the AVHRR Chs. 1-2 reflectances and ratios, the brightness temperature differences between Chs. 4 and 5, and the 4 brightness temperatures. Clear pixels are first separated from cloudy pix which are then classified into three types: cirrus, cirrus/low cloud, and cloud. This scheme has been applied to the NOAA satellite data collected over FIRE-II-IFO area, Kansas, during nine overpasses within seven observation d (November - December 1991). We have validated the detection results against cloudy conditions inferred from the collocated and coincident ground-based lida radar images, balloon-borne replicator data, and NCAR-CLASS humidity sounding a case-by-case basis. We show that the satellite detection results are consis with the cloudy conditions inferred from these independent and complemer measurements. We have also modified our retrieval scheme for the determinati cirrus optical depth and ice crystal size in multilayer cirrus cloud systems case study using FIRE-II-IFO data is reported.

1. INTRODUCTION

Cirrus clouds have been recognized to play a key role in the global radiative energy balance and climate change (Liou 1986). Information on cirrus cloud parameters is critically important to the development of cirrus cloud formation models, the upgrade of real-time global cloud analyses, and the computation of atmospheric and surface radiative parameters in climate and general circulation models.

In recent years, our research group has developed a novel and comprehensive remote sensing algorithm for the retrieval of cirrus cloud temperature, optical depth, and mean effective ice crystal size using AVHRR data (Ou et al. 1993; Rao et al. 1995). Validation of this cirrus remote sensing program has been carried out using the local daytime satellite data collected during FIRE-I-IFO and FIRE-II-IFO (Rao et al. 1995; Ou et al. 1995a). A very important procedure in determining cirrus cloud parameters is the detection of the sky condition within the field-of-view of satellite radiometers. Our detection and retrieval schemes have been developed primarily for applications to single-layer cirrus clouds.

Surface observations show that multilayer clouds frequently occur in the frontal areas where cirrus clouds overlay boundary layer convective or stratus clouds. In this paper, we describe a numerical scheme for detecting multilayer cirrus pixels using AVHRR Chs. 1 (0.63 μm), 2 (0.86 μm), 4 (10.9 μm), and 5 (12.0 μm) data. Moreover, we also present a preliminary investigation for the retrieval of cirrus cloud optical depth and ice crystal size in multilayer cloudy conditions. Verifications of the detection as well as retrieval schemes utilize the composite data sources available from FIRE-II-IFO.

2. DETECTION AND RETRIEVAL OF MULTILAYER CIRRUS CONDITIONS

2.1 DETECTION

During daytime, with the availability of visible channel data, differentiation between clear and cloudy conditions over various types of surfaces can be made using the following criteria. First, the AVHRR Ch. 1 reflectance must be less than a threshold value as a necessary condition for the presence of clear pixels. Second, we can define a ratio $Q = r_2/r_1$, where r_2 and r_1 are reflectances for Chs. 2 and 1, and use two thresholds Q_1 and Q_2, determined from the Q histograms, to identify cloudy and clear pixels over land and water surfaces, respectively. Third, the Ch. 4 brightness temperature for a clear pixel must be higher than that for a cloudy pixel so that a threshold temperature can be established for identification. Fourth, over clear regions, because of the behavior of Planck functions and atmospheric transmissions for Chs. 4 and 5 the brightness temperature difference is less than a prescribed value. We find that the preceding four criteria that use visible radiances and IR brightness temperatures are necessary and sufficient to identify the clear condition.

After all the cloudy pixels are identified, they are further classified into three classes: cirrus, cirrus/low cloud, and low cloud. First, we use the Ch. 4 brightness temperatures to detect optically thick cirrus clouds. Pixels with temperatures less than 233 K are identified as thick cirrus. Second, the visible-channel reflectances for low clouds are generally larger than those for cirrus clouds because the former are composed of water droplets with relatively small sizes and high number concentrations and are generally optically thicker than the latter (Liou 1992, Table 4.2). For this reason, a visible-channel threshold (~ 0.2) can be established to filter out those pixels that contain low clouds. Third, the Q-ratio for low clouds is usually smaller than the Q-ratio for cirrus clouds. For cirrus over land this ratio is larger than that for cirrus over low clouds. Moreover, the Q-ratio for cirrus over water is smaller than that for cirrus over low clouds. Thus, we can set threshold values to separate cirrus from either low cloud or cirrus/low cloud.

The preceding three criteria are used to separate single layer cirrus from cirrus/low cloud and low cloud alone conditions. Finally, we establish a threshold for the brightness temperature difference between Chs. 4 and 5 to differentiate the presence of nonblack cirrus overlapping low cloud and black low cloud. Moreover, the Ch. 4 brightness temperature can also be used to separate cirrus/low cloud and low cloud, because the latter temperature must be higher than about 253 K. More detailed descriptions of the detection scheme are presented in Ou et al. (1995b).

2.2 PRELIMINARY RETRIEVAL

Retrieval of the cirrus cloud optical depth and ice crystal size in multilayer cirrus condition using the AVHRR 0.63, 3.7, and 10.9 μm channels follows the numerical procedures developed by Ou et al. (1993), Rao et al. (1995), and Ou et al. (1995a). In brief, the 3.7 and 10.9 μm thermal radiances are used to retrieve the cloud temperature and emissivity from which the ice crystal size and optical depth can be determined on the basis of cloud microphysics and radiative transfer parameterizations. Removal of the solar component in the 3.7 μm radiance for applications to daytime satellite data is then made by correlating the 3.7 μm (solar) and 0.63 μm reflectances. The numerical scheme is primarily developed for single cirrus cloud systems. Validation of the algorithm has been performed by using various datasets that were collected during FIRE-II-IFO.

We have modified the preceding retrieval program to include the presence of low cloud. If its area coverage is larger than cirrus, then the upwelling radiances reaching the cirrus cloud base can be determined from the statistical histogram analyses similar to the single-layer cirrus case. The low cloud albedo can also be determined from the visible radiance for input to the removal-retrieval program developed by Rao et al. (1995). However, if both cirrus and low clouds have the

same coverage, information of the thermal upwelling radiances in the 3.7 and 10.9 μm channels as well as the low cloud albedo is unknown and must be assumed a priori. In this case, we use the climatological microphysics data for stratus to perform theoretical calculations to obtain the required inputs in retrieving the cirrus optical depth and ice crystal size. We can then compute the visible radiances at the top of the atmosphere and compare with observed radiances to assess the reliability of the calculated optical depth for low cloud. Subsequently, iterations can be developed to derive a consistent set of optical depths for both cirrus and low clouds.

3. VALIDATION OF THE DETECTION AND RETRIEVAL SCHEMES USING FIRE-II-IFO DATA

The FIRE-II-IFO was carried out near Coffeyville, Kansas, during November and December 1991. There were a number of dates during which multilayer cloudy conditions occur. For the detection of cirrus cloud pixels, the high-resolution (HRPT) AVHRR data from NOAA-11 and NOAA-12 polar-orbiting satellites are used. We have acquired ground-based lidar and radar images, balloon-borne replicator data, and NCAR-CLASS humidity soundings on a case-by-case basis. From the available datasets, we have selected seven representative dates (nine overpasses) for our study, including clear, cirrus, and cirrus/low cloud conditions. For each case, we compare cloud types identified from satellite radiances with those derived from ground-based composite instruments.

Table 1 summarizes the results of the comparisons. Columns 2-6 list the required parameters for numerical processing determined from satellite data, while columns 7-11 depict cloudy conditions obtained from satellite data and various ground-based and in situ instruments. Overall, the satellite detection scheme successfully differentiates among clear (12/6b), cirrus (11/26b and 12/5b), and cirrus/low cloud conditions. These results are consistent with the cloudy conditions identified from the independent and complementary ground-based measurements.

We have selected the cirrus/low case that occurred on 29 November 1991 for testing the retrieval scheme. Figure 1(a) displays the temperature and relative humidity profiles obtained from the NCAR-CLASS sounding launched at 1343 UTC. The cirrus cloud base and top heights derived from the replicator, PSU 94 GHz cloud radar, and visible lidar are ~ 6(-20° C) and 9 km (-41° C), respectively. A moist layer roughly corresponding to the cirrus cloud layer is evident. Moreover, another moist layer (RH > 90 %) existed between ~ 1 and 2 km, corresponding to a low-level cloud layer detected by the PSU radar. Temperature inversion occurred at the low-level cloud top and near the peak of the relative humidity around 7 km. The mean retrieved cloud temperature is 233 K, which is the average of 62 pixels within the 0.1° x 0.1° area. The standard deviation is 5.8 K, indicating that cloud temperatures were not uniform within the retrieval domain. Moreover, the mean cloud height determined from the temperature sounding is 9.2 km, which is near the cloud top.

On 29 November 1991, there were only three levels of replicator measurements available. At 9.13 km, ice particles are composed of bullet rosettes, columns, and irregular crystals with the maximum dimensions ranging from 25 to 425 μm. The size distribution peaks at 75 μm with a number concentration of 0.24 L^{-1} μm^{-1}. At 8.18 km, the ice crystal size distribution is similar to that at 9.13 km. However, the upper limit of the measured sizes increases to 575 μm. The size distribution also peaks at 75 μm, but with a smaller value of number concentration of 0.1 L^{-1} μm^{-1}. The level at 7.46 km corresponds to a local peak in the relative humidity profile. The size distribution with a upper limit of 875 μm is broader than the previous two. The ice crystal shapes include bullet rosettes and aggregates. The derived mean effective sizes for these three levels are 96, 116, and 146 μm from top to bottom. The vertically averaged mean effective ice crystal size is 134.6 μm (solid vertical bar in Fig. 1b). The retrieved mean effective size from satellite radiances is

130.9 μm. On the bottom scale are shown the replicator derived and the satellite retrieved optical depths, which are 2.21 and 2.44, respectively.

We are in the process of improving and refining the retrieval program for the determination of cirrus optical depth and mean ice crystal size. More comprehensive analyses and validations will be reported in the future.

4. ACKNOWLEDGEMENTS

This work was supported by the Air Force Geophysics Directorate Contract F19628-95-K-002 and NASA Grants NAG5-1050 and NAG1-1719.

REFERENCES

Liou, K.N., 1986: Influence of cirrus clouds on weather and climate processes: A global perspective. Mon. Wea. Rev., 114, 1167-1199.

Liou, K.N., 1992: Radiation and Cloud Processes in the Atmosphere: Theory, Observation, and Modeling. Oxford University Press, New York, 487 pp.

Ou, S.C., K.N. Liou, W.M. Gooch, and Y. Takano, 1993: Remote sensing of cirrus cloud parameters using advanced very-high resolution radiometer 3.7 and 10.9 μm channels. Appl. Opt., 32, 2171-2180.

Ou, S.C., K.N. Liou, Y. Takano, et al., 1995a: Remote sounding of cirrus cloud optical depths and ice crystal sizes from AVHRR data: Verification using FIRE-II-IFO measurements. J. Atmos. Sci., FIRE-II Special Issue (accepted and in press).

Ou, S.C., K.N. Liou, and B. Baum, 1995b: Detection of multilayer cirrus cloud systems using AVHRR data: Verification based on FIRE-II-IFO composite measurements. J. Appl. Meteor., (accepted and in press).

Rao, N.X., S.C. Ou, and K.N. Liou, 1995: Removal of the solar component in AVHRR 3.7 μm radiances for the retrieval of cirrus cloud parameters. J. Appl. Meteor., 34, 482-499.

Table 1. Results of the satellite-based cloud detection compared with ground-based radar, lidar, and balloon-borne replicator measurements.

r_1: Ch. 1 reflectance
Q: Ratio of Ch. 2 to Ch. 1 radiances
BTD45: Brightness temperature difference between Ch. 4 and Ch. 5
T_4: Ch. 4 brightness temperature
a: NOAA-12 overpass (~ 1400 UTC)
b: NOAA-11 overpass (~ 2100 UTC)

Date	Parameter Values					Cloudy Condition				
	number of pixels	r_1(%)	Q	BTD45(K)	T_4(K)	satellite	PSU radar	ETL lidar*	LaRc lidar*	soundings
12/6b	117	12.1	1.22	0.92	287.0	clear	clear	clear	clear	----/dry
12/5b	89	32.1	1.07	3.04	249.4	cirrus	cirrus	cirrus	cirrus	ice/dry
11/26b	79	24.2	1.10	2.73	271.6	cirrus	cirrus	cirrus	cirrus	ice/dry
11/22a	93	57.7	0.91	0.46	244.7	ci/low	ci/low	cirrus	cirrus	ice/low
11/29a	52	45.6	0.89	1.18	249.7	ci/low	ci/low	------	------	ice/low
11/28a	100	23.8	0.91	2.09	272.1	ci/low	ci/low	cirrus	cirrus	ice+/low
11/28b	85	20.0	1.04	1.77	284.2	cirrus	cirrus	cirrus	cirrus	ice+/dry
11/27a@	5200	44.5	0.91	0.80	246.0	ci/low	ci/low	------	------	----/low
11/27b	67	63.5	0.93	3.74	262.7	ci/low	ci/low	------	------	----/low

*: Both ETL lidar and LaRc lidar measured signals from the backscattering of boundary layer aerosols and low cloud particles. These signals were not included in the images analyzed in this study.
+: Based on replicator measurements between the two satellite overpasses.
@: Satellite cloud detection results are based on data over 1.0°x1.0° area around 38.5° N, 96.5° W.

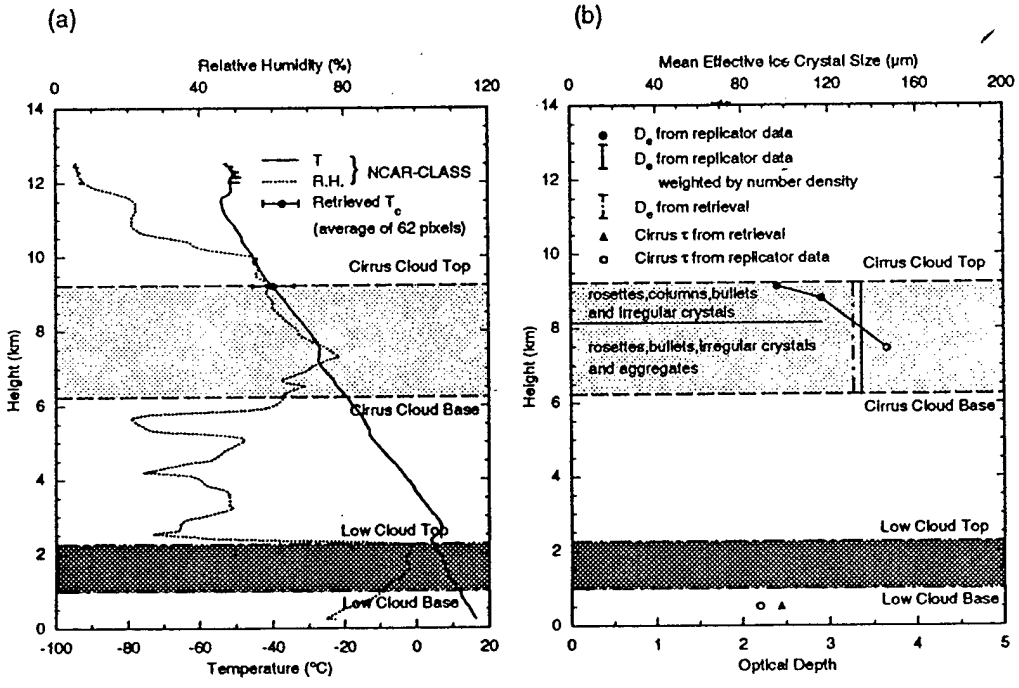

Figure 1. (a) Cloud base and top heights for cirrus and stratus determined from lidar, radar and sounding data, as well as temperature and humidity profiles obtained from the NCAR CLASS sounding system at 1343 UTC, 29 November 1991. Overlapped with the temperature profile are the mean retrieved cirrus cloud temperature over 0.1° x 0.1° domain around Coffeyville, Kansas, and (b) Display of the replicator-derived mean effective sizes at selected height levels, their vertical average, and the retrieved value. Also shown on the bottom scale are the optical depths derived form the replicator data and from the retrieval.